ORIGINAL ARTICLE

Plasma Ceramides in Relation to Coronary Plaque Characterization Determined by Optical Coherence Tomography

Weili Pan[1,2] · Hui Dong[1,2] · Rong Sun[1,2] · Linlin Zhao[1] · Meng Sun[1,2] · Longyan Li[3] · Xianghao Yu[1,2] · Jinxin Liu[1,2] · Jianjun Wu[1,2] · Fan Yang[1,2] · Bo Yu[1,2]

Abstract

Plasma ceramides (Cer), a subset of bioactive lipids, have mechanistic links to development of atherosclerosis and are related to major adverse cardiovascular events (MACEs). Previous researches have demonstrated vulnerable plaques contribute to acute cardiovascular events and poor prognosis. This study aimed to explore the associations between Cer and culprit plaque characterizations evaluated by optical coherence tomography (OCT). It was found that plasma Cer are associated with culprit plaque vulnerability evaluated by OCT, providing evidence supporting proatherogenic roles and potential to act as markers for plaque vulnerability of Cer.

Keywords Plasma ceramides · Plaque vulnerability · STEMI · *RRLC-Q-TOF/MS*

Abbreviations

Cer	Ceramide
CHD	Coronary heart disease
STEMI	St-segment elevation myocardial infarction
OCT	Optical coherence tomography
PR	Plaque rupture
LRP	Lipid-rich plaque
TCFA	Thin-cap fibroatheroma
FCT	Fibrous cap thickness
RRLC-Q-TOF/MS	Rapid resolution liquid chromatography coupled with quadrupole time-of-flight mass spectrometry
MACEs	Major adverse cardiovascular events
Hs-CRP	High-sensitive c-reactive protein
TC	Total cholesterol
TG	Triglyceride
HDL-C	High-density lipoprotein cholesterol
LDL-C	Low-density lipoprotein cholesterol

Associate Editor Craig M. Stolen oversaw the review of this article

✉ Bo Yu
dryu_hmu@163.com

1 Department of Cardiology, The Second Affiliated Hospital of Harbin Medical University, Harbin, Province Heilongjiang, China

2 The Key Laboratory of Myocardial Ischemia, Chinese Ministry of Education, Harbin, Province Heilongjiang, China

3 Department of Cardiology, People's Liberation Army Joint Logistics Support Unit 962 Hospital, Harbin, Province Heilongjiang, China

Introduction

Ceramides (Cer), a key sphingolipid product of sphingomyelinase (SM), are an integral part of the cell membrane of eukaryotes. They contribute to the structural stability of the cell and act as bioactive lipids in various cell signalling pathways including apoptosis, inflammation and cell cycle arrest [1]. It has been acknowledged that Cer play critical roles in development and progression of atherosclerosis in recent years [2–4]. A substantial body of literature in rodent models of cardiovascular disease and a well-known randomized trial (PREDIMED trial) indicate that Cer play causative roles in coronary artery disease (CAD) [5–7]. Moreover, recent studies have validated that plasma Cer can predict major adverse cardiovascular events (MACEs) in patients with CAD, even beyond low-

density lipoprotein (LDL) cholesterol, and that Cer molecules (Cer (d18:1/16:0), Cer(d18:1/18:0) and Cer(d18:1/24:1)) and Cer(d18:1/24:0) have the closest connection with MACEs among all Cer species [8–10]. However, association between plasma MACEs-related Cer and culprit plaque characteristics have not been clearly elucidated.

Optical coherence tomography (OCT) is called "optical biopsy" due to its high resolution, which is able to accurately evaluate culprit lesion characteristics in vivo [11]. Previous OCT researchers have confirmed that thin-cap fibroatheroma (TCFA), plaque rupture (PR), macrophage infiltration, cholesterol crystal and microchannel have a positive relationship with plaque vulnerability, while calcification has a negative relationship with plaque vulnerability [12, 13]. This study aimed to explore the associations between plasma MACE-related Cer concentrations and culprit plaque characterizations evaluated by OCT in patients with ST segment myocardial infarction (STEMI). We found that plasma Cer are related with culprit plaque vulnerability and strong and independent predictors for TCFA in STEMI patients.

Methods and Materials

Study Design and Population

We retrospectively enrolled 312 consecutive patients first diagnosed with STEMI and undergoing an OCT examination before interventional procedures at the 2nd Affiliated Hospital of Harbin Medical University between July 2017 and December 2017. STEMI was diagnosed, and culprit lesions characteristics were confirmed according to previous criteria [14]. All the STEMI patients were admitted within 12 h of symptom onset, and blood withdrawals were completed before intervention procedures. Patients with coronary bypass grafts, congestive heart failure, end-stage renal disease, and serious liver dysfunction were excluded. Additionally, those who were not available for an OCT examination because of left main disease, chronic total occlusion, or extremely tortuous or heavily calcified vessels were also not included. Two hundred and forty-nine eligible patients and a specific study flow chart is shown in Fig. 1. In addition, we screened 30 healthy donors without known cardiovascular disease as plasma Cer levels references. The current study was approved by the Ethics Committee of the 2nd Affiliated Hospital of Harbin Medical University (Harbin, China), and all patients provided written informed consent.

Optical Coherence Tomography Image Acquisition and Analysis

Patients were administered 300 mg aspirin, 600 mg clopidogrel or 180 mg ticagrelor and unfractionated heparin (100 IU/kg) prior to interventional procedures.
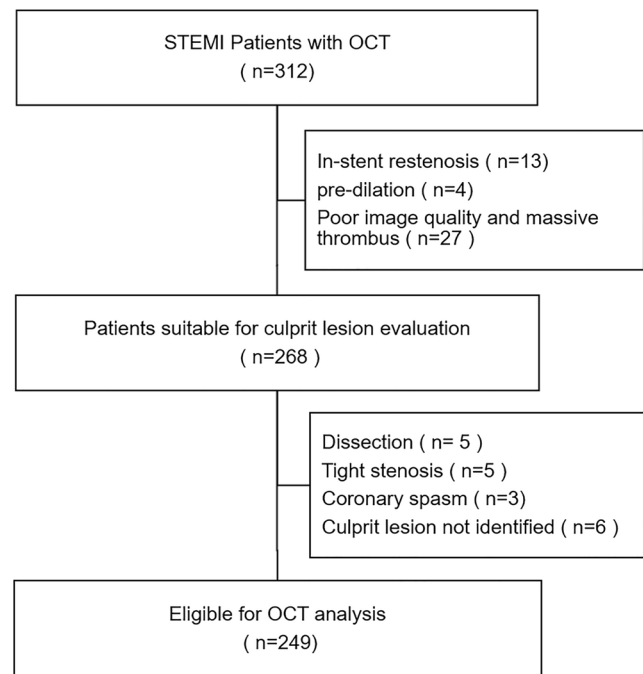

Fig. 1 Study flow chart. OCT, optical coherence tomography; STEMI, ST segment elevation myocardial infarction

Aspiration thrombectomy was applied to reduce the thrombus burden before the OCT examination. The frequency domain ILUMIEN OPTIS OCT system was used in this study to acquire OCT images of the culprit lesions.

All OCT images were analysed by two experienced investigators blinded to other experimental data on the ILUMIEN OPTIS OCT Offline Review Workstation. Consistent with previous diagnostic criteria [15], a lipid-rich plaque (LRP) was defined as a lipid plaque with lipid arc more than 180° in any cross-section (Fig. 3a); a TCFA was defined as a LRP with the thinnest fibrous cap < 65 μm (Fig. 3b); plaque rupture (PR) was characterized by the presence of fibrous cap discontinuity with cavity formation (Fig. 3c); macrophages accumulation was defined as signal-rich, distinct or confluent punctuate regions with heterogeneous backward shadowing (Fig. 3d); a microchannel was defined as a black hole with diameter of 50–300 μm on multiple contiguous frames; cholesterol crystal was signal-rich, thin and linear region (Fig. 3e); calcification was defined as well-delineated, signal poor regions with sharp borders (Fig. 3f); a calcification with arc < 90° and length < 4 mm was defined as microcalcification. Additionally, lipid core length was recorded on the longitudinal OCT view. For each lipid plaque, the lipid arc was measured at every 1-mm interval throughout the entire lesion, and fibrous cap thickness (FCT) was measured at its thinnest part 3 times, and the average value was calculated. Lipid volume index was calculated by multiplying lipid core length by mean lipid-rich arch.

The inter-observer kappa coefficients for PR, TCFA, LRP and calcification were 0.887, 0.891, 0.875 and 0.885,

142

J. of Cardiovasc. Trans. Res. (2021) 14:140–149

respectively. The intra-observer kappa coefficients for PR, TCFA, LRP and calcification were 0.905, 0.917, 0.905 and 0.898, respectively.

Preparation of Human Plasma Samples

Blood samples (5 ml) were collected before intervention using EDTA tubes. Plasma samples were separated by centrifugation at 1000 g for 10 min and then stored at -80 °C until further analysis. Quality control (QC) consisted of mixture of 2 μl from each study sample. Cer extraction was performed according to previous descriptions [16, 17] with minor modifications. In brief, 150 μl of study samples and QC samples were deproteinated with 450 μl cold isopropanol, vortexed for 1 min and then incubated at -80 °C for 1 h. Next, the samples were centrifuged at 16,000 g at 4 °C for 20 min, and 500 μl of supernatant was transferred to a 1.5-ml EP tube. A total of 40 μl of the supernatant was diluted (2:1, v/v) with H2O/ methanol (1:1, v/v) containing D7-labelled internal standard (IS) mix (Avanti Polar Lipids, Alabaster, AL). IS mix solution containing D7-Cer d18:1/16:0 (0.5 ng/μl), D7-Cer d18:1/18:0 (0.5 ng/μl), D7-Cer d18:1/24:0 (2 ng/μl) and D7-Cer d18:1/24:1 (3.3 ng/μl) was prepared in methanol.

Quantitative Analysis of Cer Using Rapid Resolution Liquid Chromatography Coupled with Quadrupole Time-of-Flight Mass Spectrometry

Chromatographic separation was performed at 60 °C on an Agilent Technologies 1260 liquid chromatography system. The mobile phases consisted of water (A) and isopropanol (B). Gradient elution was maintained at 85% B for 4 min. The type of RRLC column was ZORBAX SB-C18 (Rapid Resolution HT, 4.6×50 mm, 1.8 μm), and the injection volume was 10 μl. Mass spectrometric analysis was performed on an Agilent 6530 series quadrupole time-of-flight mass spectrometer equipped with a dual electrospray ionization source (ESI). Ionization was operated in positive (ESI+) mode. The chosen m/z values were 560.5028/567.5471 for Cer(d18:1/16:0)/D7-Cer(d18:1/16:0), 588.5346/595.5783 for Cer(d18:1/18:0)/ D7-Cer(d18:1/18:0), 670.6136/677.6548 for Cer(d18:1/ 24:1)/D7-Cer(d18:1/24:1) and 672.6276/679.6723 for Cer (d18:1/24:0)/D7-Cer(d18:1/24:0). Retention time (RT) for Cer(d18:1/16:0), Cer(d18:1/18:0), Cer(d18:1/ 24:1) and Cer (d18:1/24:0) is 1.680 min, 1.898 min, 2.521 min and 2.893 min, respectively. Chromatograms of the four Cer were shown in supplementary files Figure 1.

QC samples were measured after every 30 study samples, and determinations of Cer concentrations in all QC samples were performed to evaluate the inaccuracy of Cer arrays by the Bessel formula. The analytic imprecision values for Cer(d18:1/16:0), Cer(d18:1/18:0), Cer(d18:1/24:1) and Cer(d18:1/24:0)) were 5.25%, 4.98%,7.43% and 8.89%, respectively.

Statistical Analysis

Based on the Kolmogorov–Smirnov test, continuous data are expressed as the mean ± standard deviation or the median ± interquartile range and were analysed with Student's t test or a nonparametric test, respectively. Categorical variables are presented as a number (percent) and were compared with chi-square tests or Fisher's exact test. Spearman analysis was performed to evaluate the correlation between plasma Cer and quantitative OCT parameters. Logistic regression analysis was performed to determine the odds ratio and 95% confidence interval (CI) for TCFA. Adjustments were made for variables including age, gender, hypertension, diabetes, cigarettes smoking, high-sensitive C-reactive protein (hs-CRP), total cholesterol (TC), triglyceride (TG), high-density lipoprotein cholesterol (HDL-c), low-density lipoprotein cholesterol (LDL-c), admission creatinine, thrombectomy, multiple-vessel disease and previous medication use (including statin, antiplatelet drugs, β-blocker, ACEI/ARE and CCB) in the multivariate logistic regression analysis. The Bessel formula was used to evaluate the inaccuracy of the plasma Cer measurements. All tests were two-sided, and a P value of < 0.05 was considered statistically significant. All statistical analyses were performed using the SPSS 23.0 software (IBM, Armonk, New York, USA).

Results

Characteristics of Patients and Plasma Ceramide Levels

We screened 312 STEMI patients with OCT examination and 30 healthy donors. Of the 312 STEMI patients, 63 were excluded (as shown in Fig. 1). A total of 249 patients were eligible for culprit plaque characteristics analysis. Circulating Cer levels were higher in patients with STEMI than in healthy donors (as shown in Fig. 2). Baseline clinical characteristics and plasma MACE-related Cer levels (Cer(d18:1/16:0), Cer(d18:1/18:0), Cer(d18:1/24:1) and Cer(d18:1/24:0)) in STEMI patients were shown in Table 1, and those in healthy donors were shown in supplementary files Table 1. Moreover, detailed OCT characteristics of culprit plaques in screened patients were shown in Table 2.

Fig. 2 Comparison of plasma ceramide concentrations in different cohorts. **a** Comparison of plasma Cer(d18:1/16:0) levels in healthy controls vs. patients with STEMI. **b** Comparison of plasma Cer(d18:1/18:0) levels in healthy controls vs. patients with STEMI. **c** Comparison of plasma Cer(d18:1/24:1) levels in healthy controls vs. patients with STEMI. **d** Comparison of plasma Cer(d18:1/24:0) levels in healthy controls vs. patients with STEMI
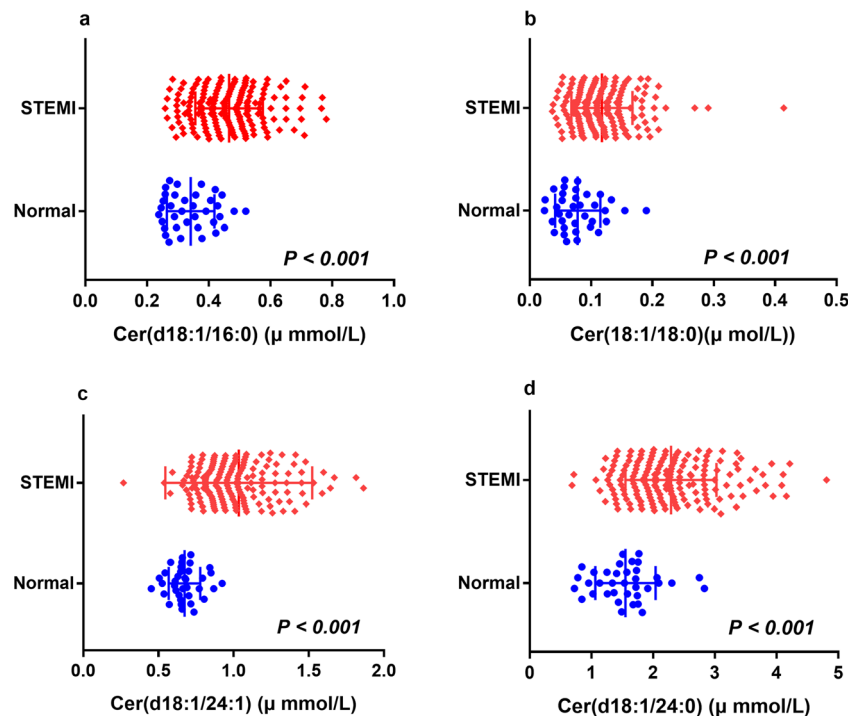
Correlation Between Plasma Ceramides and Culprit Plaque Characteristics Determined by Optical Coherence Tomography

All eligible STEMI patients were stratified by median of plasma Cer concentrations. The prevalence of LRP, PR and TCFA was higher in high Cer group than that in low Cer group, while the frequency of calcification was lower in high Cer group (as shown in Table 3 and Fig. 3). Moreover, the frequency of microstructure (including macrophages infiltration, cholesterol crystal, microchannel and microcalcification) was similar between the low Cer group and the high Cer group (as shown in Table 3 and Fig. 3). Similarly, patients in high Cer group had longer lipid core length, larger mean lipid arc, bigger lipid volume index and thinner FCT than patients in low Cer group (as shown in Table 3).

In addition, the Spearman analysis showed that plasma Cer(d18:1/16:0) Cer(d18:1/18:0) and Cer(d18:1/24:1) have significant positive correlations with lipid core length, mean lipid arc and lipid volume index, a significant negative correlation with FCT (as shown in Table 4).

Predictive Value of Plasma Ceramides for Thin-Cap Fibroatheroma

Clinical characteristics of STEMI patients grouped by TCFA (+) were shown in supplementary files Table 2.

The univariate regression analysis showed that four MACEs-related plasma Cer were all predictors for TCFA (as shown in Table 5). Moreover, Cer(d18:1/16:0), Cer(d18:1/18:0) and Cer(d18:1/24:1) (except for Cer(d18:1/24:0)) remained strongly and independently associated with the presence of TCFA even after adjusting for age, gender, hypertension, diabetes, cigarettes smoking, hs-CRP, TC, TG, HDL-c, LDL-c, admission creatinine, thrombectomy, multiple-vessel disease and previous medication use (including statin, antiplatelet drugs, β-blocker, ACEI/ARE and CCB) (as shown in Table 5).

Discussion

There is a significant increase in plasma Cer levels from healthy individuals to patients with STEMI in this study. This is consistent with previous study, suggesting Cer are important atherogenic substances and associated with all degrees of CAD [1, 18, 19]. Additionally, this study demonstrated for the first time that plasma Cer are associated with culprit plaque vulnerability evaluated by OCT. Even after adjusting for traditional risk factors, elevated Cer(d18:1/16:0), Cer(d18:1/18:0) and Cer(d18:1/24:1) (except for Cer(d18:1/24:0)) can still serve as an independent predictor for TCFA in STEMI patients, suggesting elevated plasma Cer may represent a marker of coronary

Table 1 Basic characteristics of patients

Variables	Overall ($n = 249$)
Age, years	56.78 ± 12.84
Men (%)	186 (74.70)
Coronary risk factors	
Hypertension	120 (48.19)
Diabetes mellitus	42 (16.86)
Cigarettes smoking	
Non- smoker	103 (41.37)
Current smoker	135 (54.21)
Former smoking	11 (4.42)
Laboratory data	
Creatinine (μ mmol/L)	84.95 ± 23.5
hs-CRP (mg/L)	8.35 ± 9.85
TC (mg/dL)	180.71 ± 39.58
Triglyceride (mg/dL)	149.04 ± 86.73
HDL-C (mg/dL)	48.60 ± 10.23
LDL-C (mg/dL)	108.21 ± 32.57
Procedural characteristics	
Multi-vessels disease	184 (73.89)
Total ischemic time (h)	5.28 ± 4.00
Infarction-related artery	
LAD (%)	127 (51.00)
RCA (%)	92 (36.95)
LCX (%)	30 (12.05)
Previous medication use	
Statins use (%)	28 (11.24)
Antiplatelet drugs (%)	30 (13.65)
β-blocker (%)	10 (4.02)
ACEI/ARE (%)	25 (10.04)
CCB (%)	90 (36.14)
Ceramides concentration:	
Cer(d18:1/16:0) (μ mol/L)	0.45 ± 0.11
Cer(d18:1/18:0) (μ mol/L)	0.12 ± 0.05
Cer(d18:1/24:1) (μ mol/L)	0.99 ± 0.42
Cer(d18:1/24:0) (μ mol/L)	2.19 ± 0.69

Values are presented as n (%), mean ± SD, or median ± interquartile range. *Cer*, ceramides; *TCFA*, thin-cap fibroatheroma; *LAD*, left anterior descending artery; *RCA*, right coronary artery; *LCX*, left circumflex artery; *MI*, myocardial infarction; *ACEI*, angiotensin-converting enzyme inhibitors; *ARB*, angiotensin receptor blocker; *CCB*, calcium channel blockers

Table 2 OCT characteristics of culprit plaques in patients

Variables	Overall ($n = 249$)
Qualitative OCT analysis	
LRP	202 (81.8)
PR	175 (70.3)
TCFA	185 (74.3)
Macrophages	206 (82.7)
Cholesterol crystal	154 (62.8)
Microchannel	79 (31.7)
Calcification	30 (12.0)
Microcalcification	88 (35.3)
Quantitative OCT analysis	
Lipid core length (mm)	11.71 ± 9.20
Mean lipid arc (°)	212.34 ± 66.16
Lipid volume index	2686.36 ± 2398.31
FCT (mm)	94.38 ± 42.09
MLA (mm^2)	1.55 ± 0.66

Values are presented as n (%), mean ± SD, or median ± interquartile range. *Cer*, ceramides; *OCT*, optical coherence tomography; *LPR*, lipid-rich plaque; *PR*, plaque rupture; *TCFA*, thin-cap fibroatheroma; *FCT*, fibrous cap thickness; *MLA*, minimal lumen area

disease activity and paly critical roles in progression of atherosclerosis (Fig. 4).

Previous studies have confirmed that Cer are important atherogenic substances and have a close connection with many well-known risks of cardiovascular disease, such as lipoproteins, inflammatory cytokines and matrix metalloproteinases (MMPs) [18]. The present study sheds light on the relationship between plasma-specific Cer and culprit plaque vulnerability in STEMI patients. The exact mechanisms by which plasma Cer lead to plaque instability are not clearly known. However, preliminary experimental data can partially explain this phenomenon. Schissel et al. found that increased Cer can activate sphingomyelinase, which is able to induce lipoproteins, especially LDL-C, to aggregate and accumulate in the arterial wall [20]. The greater accumulation of LDL-C in the arterial wall makes the lipid plaques larger and more prone to be unstable. Moreover, the development and progression of vulnerable plaques are tightly related to the inflammatory response and MMPs [21]. Some studies have demonstrated that Cer signalling is a crucial mediator in the proinflammatory effects and activation of MMPs. Furthermore, Andreas was the first to validate that Cer play an pivotal role in the proinflammatory effect and in inducing human coronary artery smooth muscle cell (HCASMC) apoptosis/necrosis in vitro [2]. Interestingly, the loss of vascular smooth muscle cells (VSMCs) is a major player in the progression of vulnerable plaque, leading to a thinner fibrous cap [22, 23]. Additionally, Cer are primarily responsible for endothelial dysfunction by inducing oxidative stress and reducing nitric oxide (NO) bioavailability from endothelial cells [24]. These evidence supports the significance of Cer in plaque vulnerability with respect to their associations

Table 3 Optical coherence tomography analysis

Variables	Cer(d18:1/16:0) level			Cer(d18:1/18:0) level			Cer(d18:1/24:1) level			Cer(d18:1/24:0) level		
	Low (n=124)	High (n=125)	P value	Low (n=124)	High (n=125)	P value	Low (n=124)	High (n=125)	P value	Low (n=124)	High (n=125)	P value
Qualitative OCT analysis												
LRP	96 (77.4)	106 (84.8)	0.048	96 (77.4)	106 (84.8)	0.048	96 (77.4)	106 (84.8)	0.048	96 (77.4)	106 (84.8)	0.048
PR	75 (60.5)	100 (80.0)	0.001	79 (63.7)	96 (76.8)	0.027	79 (63.7)	96 (76.8)	0.027	80 (64.5)	95 (76.0)	0.043
TCFA	82 (66.1)	103 (82.4)	0.004	89 (71.8)	96 (76.8)	0.387	86 (69.4)	99 (79.2)	0.083	89 (71.8)	96 (76.8)	0.387
Macrophages	102 (82.3)	104 (83.2)	0.868	99 (79.8)	107 (85.6)	0.245	103 (83.1)	103 (82.4)	1.000	99 (79.8)	107 (85.6)	0.245
Cholesterol crystal	76 (61.3)	78 (62.4)	0.897	77 (62.1)	77 (61.6)	1.000	77 (62.1)	77 (61.6)	1.000	75 (60.5)	79 (63.2)	0.697
Microchannel	37 (29.8)	42 (33.6)	0.586	38 (30.6)	4 1 (32.8)	0.786	37 (29.8)	42 (33.6)	0.586	41 (33.1)	38 (30.4)	0.684
Calcification	19 (15.3)	11 (8.8)	0.124	18 (14.5)	12 (9.6)	0.249	22 (17.7)	8 (6.4)	0.006	18 (14.5)	12 (9.6)	0.249
Microcalcification	44 (35.5)	44 (35.2)	1.000	44 (35.5)	44 (35.2)	1.000	46 (37.1)	42 (33.6)	0.597	39 (31.2)	49 (39.5)	0.186
Quantitative OCT analysis												
Lipid core length (mm)	10.55±7.40	12.76±9.80	0.006	11.14±8.5	12.23±9.6	0.059	10.88±8.90	12.49±9.5	0.035	11.58±9.8	11.82±8.8	0.130
Mean lipid arc (°)	206.31±78.19	217.86±62.25	0.011	213.39±66.75	221.20±66.34	0.240	207.15±70.18	217.26±63.61	0.056	210.81±64.67	213.73±69.32	0.199
Lipid volume index	2386.50±2034.26	2960.58±2478.38	0.004	2598.75±2395.48	2766.47±2385.95	0.099	2479.21±2527.22	2882.70±2149.79	0.037	2674.34±2020.13	2699.73±2838.04	0.161
FCT (mm)	96.85±47.50	92.11±31.15	0.013	95.63±33.64	93.00±49.21	0.238	96.83±48.34	92.06±33.00	0.010	97.02±49.15	91.44±34.26	0.541
MLA (mm^2)	1.55±0.78	1.56±0.61	0.330	1.56±0.59	1.55±0.72	0.833	1.65±0.74	1.45±0.63	0.027	1.61±0.78	1.49±0.60	0.187

Values are presented as n (%), mean ± SD or median ± interquartile range. *Cer*, ceramides; *OCT*, optical coherence tomography; *LPR*, lipid-rich plaque; *PR*, plaque rupture; *TCFA*, thin-cap fibroatheroma; *FCT*, fibrous cap thickness; *MLA*, minimal lumen area

146

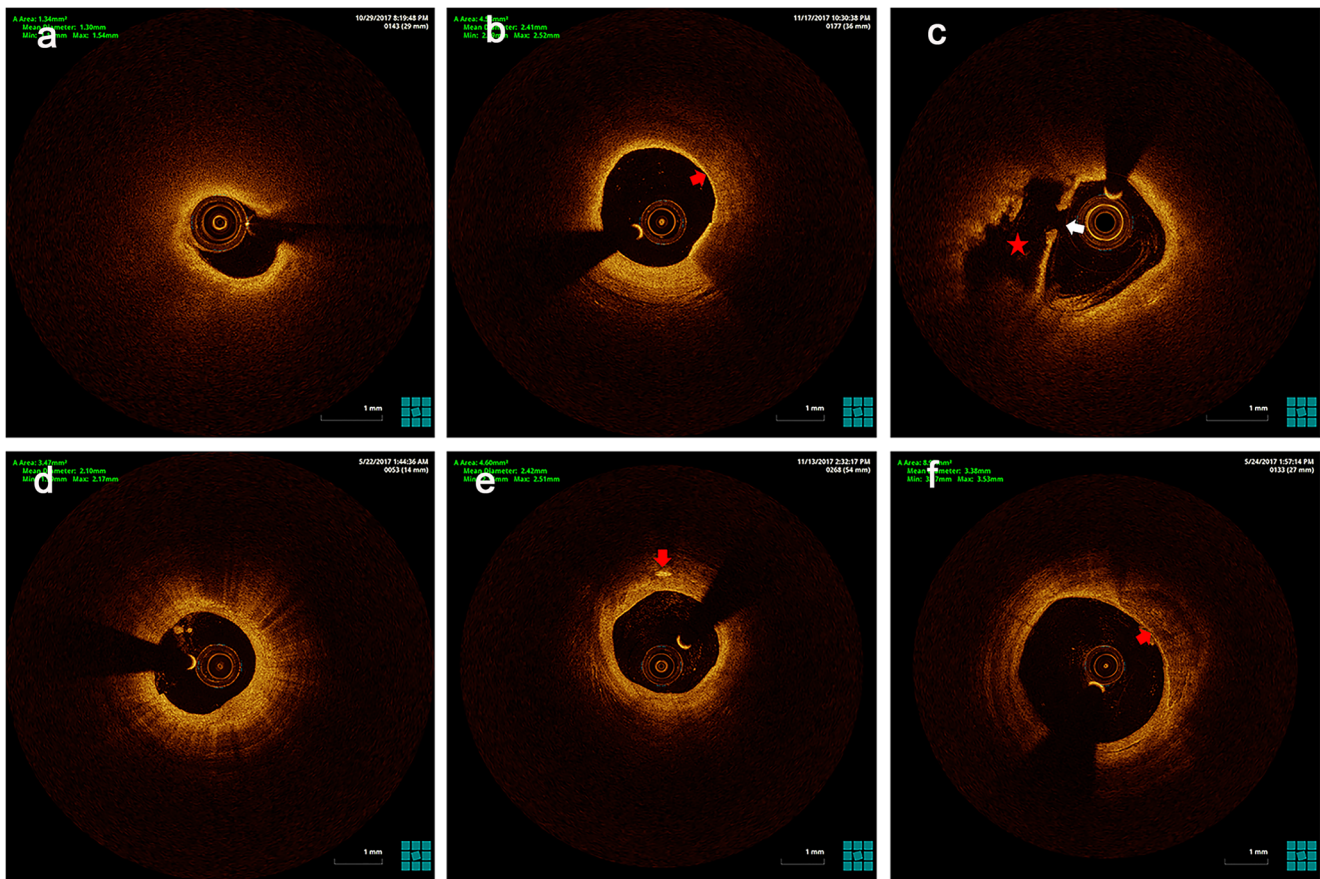J. of Cardiovasc. Trans. Res. (2021) 14:140–149

Fig. 3 Representative OCT images. **a** Lipid-rich plaque (LRP), a lipid plaque with lipid arc more than 180°. **b** A thin-cap fibroatheroma (TCFA), a lipid-rich plaque with the thinnest fibrous cap < 65 μm (the red arrow). **c** Plaque rupture (PR), presence of fibrous cap discontinuity (the white arrow) with cavity formation (the red asterisk). **d** Macrophage accumulation, signal-rich, distinct or confluent punctuate regions with heterogeneous backward shadowing. e Cholesterol crystal, signal-rich, thin and linear region (the red arrow). **f** Calcification, well-delineated, signal-poor regions with sharp borders (the red arrow).

with lipoprotein aggregation, inflammatory cytokines, MMPs, HCASMC apoptosis/necrosis and endothelial dysfunction.

In addition, plaques in patients with diabetes mellitus (DM) are more unstable than that in patients without DM [25, 26]. Interestingly, plasma Cer have been reported to be related to the development of type 2 DM, insulin resistance [27, 28]. Higher concentrations of circulating Cer(d18:1/18:0) are associated with increased risk of developing diabetes [27]. Furthermore, a significant reduction in Cer(d18:1/16:0) can improve insulin resistance and lower the incidence of diabetes mellitus [28].

Table 4 Correlation between plasma ceramides and quantitative OCT parameters

Variables	Cer(d18:1/16:0)		Cer(d18:1/18:0)		Cer(d18:1/24:1)		Cer(d18:1/24:0)	
	r	p	r	p	r	p	r	p
Lipid core length (mm)	0.175	0.006	0.187	0.003	0.131	0.039	0.124	0.049
Mean lipid arc (°)	0.144	0.023	0.169	0.008	0.168	0.008	0.054	0.397
Lipid volume index	0.171	0.007	0.185	0.003	0.148	0.019	0.108	0.089
FCT (mm)	− 0.158	0.022	− 0.123	0.067	− 0.213	0.001	− 0.123	0.067
MLA (mm^2)	0.046	0.436	0.013	0.769	0.108	0.089	0.060	0.343

OCT, optical coherence tomography; Cer, ceramides; OCT, optical coherence tomography; FCT, fibrous cap thickness; MLA, minimal lumen area

Table 5 Logistic regression analysis of ceramides for TCFA

Model	Variables	OR (95% CI)	Adjusted OR (95%CI)	*P* value
Model 1	Cer(d18:1/16:0)[a]	7.279 (2.244–23.617)	7.269 (1.773–29.801)	0.006
Model 2	Cer(d18:1/18:0)[a]	3.110 (1.513–6.389)	2.904 (1.199–7.033)	0.018
Model 3	Cer(d18:1/24:1)[a]	5.538 (1.364–22.493)	6.274 (1.350–29.154)	0.019
Model 4	Cer(d18:1/24:0)[a]	1.307 (0.855–1.966)	1.785 (0.988–3.227)	0.055

[a] Natural logarithm of the ceramides

Models 1, 2, 3 and 4. Adjusted for age, gender, hypertension, diabetes, cigarettes smoking, hs-CRP, TC, TG, HDL, LDL, admission creatinine, thrombectomy, multiple-vessel disease and previous medication use (including statin, antiplatelet drugs, β-blocker, ACEI/ARE and CCB). *TCFA*, thin-cap fibroatheroma

Some previous studies have confirmed that distinct plasma Cer are superior to traditional risk factors in predicting MACEs in patients with CAD [9, 29]. However, the underlying mechanism remains unclear. Our study can partially explain their predictive value. The present results showed that plasma Cer concentrations have positive relationship with culprit plaque vulnerability. Unstable plaques are able to increase the occurrence of adverse cardiovascular events. Our results emphasize the potential importance of Cer in plaque instability in addition to the development of CAD.

Plasma Cer are able to reflect dynamic changes in the coronary disease stability because of their modifiable nature. Importantly, the response of Cer to lipid-lowering treatments has also been documented in several previous experiments [30–32]. Traditional statins, already known to be effective at making plaques more stable and reducing the risk of CAD, are also reported to modify plasma Cer concentrations. For example, simvastatin lowers plasma Cer broadly by approximately 25%, and rosuvastatin dose-dependently lowers plasma Cer by 33–37% independent of LDL-C-lowering [31, 32]. The proprotein convertase subtilisin/kexin-type 9 (PCSK9) inhibitor, a new lipid-lowering drug, is also reported to reduce CAD outcome risk-related Cer by 20% [32].

This study is subject to several limitations. First, this was a retrospective study conducted at a single centre. Second, we screened patients with STEMI who underwent an OCT examination before percutaneous coronary intervention. Patients who were unavailable for the OCT examination were not included. Third, a residual thrombus might affect the analysis of plaque characteristics. Fourth,

Fig. 4 Prevalence of qualitative OCT parameters stratified by median of plasma Cer. **a** Prevalence of qualitative OCT parameters stratified by median of Cer(d18:1/16:0). **b** Prevalence of qualitative OCT parameters stratified by median of Cer(d18:1/18:0). **c** Prevalence of qualitative OCT parameters stratified by median of Cer(d18:1/24:1). **d** Prevalence of qualitative OCT parameters stratified by median of Cer(d18:1/24:0)

148

J. of Cardiovasc. Trans. Res. (2021) 14:140–149
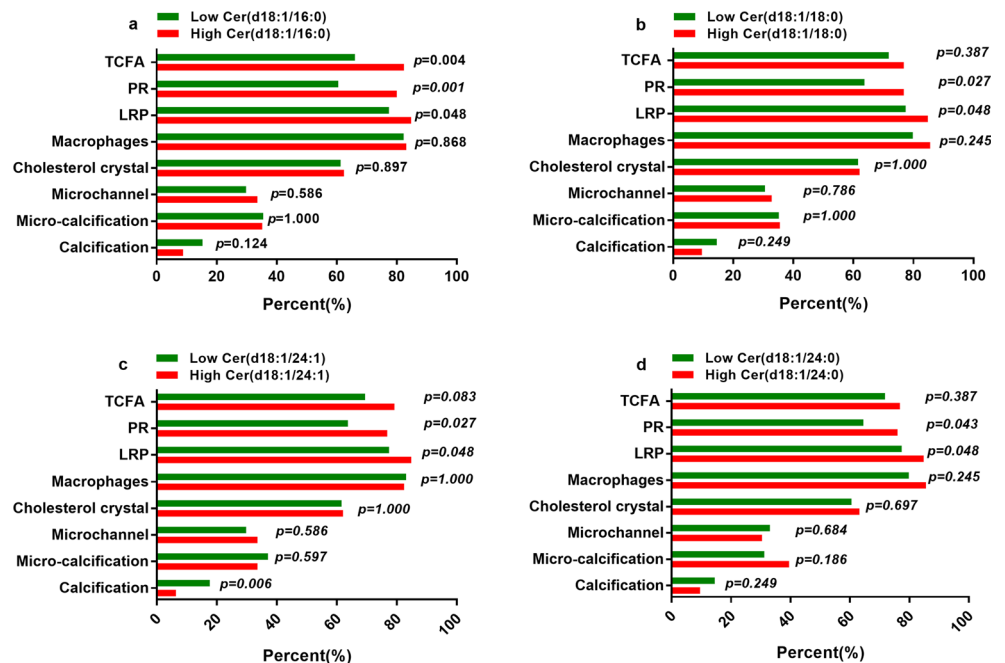
non-culprit plaques were not assessed in this study. Fifth, the peak time of plasma Cer after AMI is uncertain, so different blood collection times may affect plasma Cer concentrations.

Compliance with Ethical Standards

Conflict of Interest The authors declare that they have no conflict of interest.

Human Subjects/Informed Consent Statement All procedures followed were in accordance with the ethical standards of the responsible committee on human experimentation (institutional and national) and with the Helsinki Declaration of 1975, as revised in 2000 (5). Informed consent was obtained from all patients for being included in the study.

References

1. Stith, J. L., Velazquez, F. N., & Obeid, L. M. (2019). Advances in determining signaling mechanisms of ceramide and role in disease. *Journal of Lipid Research, 60*(5), 913–918. https://doi.org/10.1194/jlr.S092874.

2. Edsfeldt, A., Duner, P., Stahlman, M., Mollet, I. G., Asciutto, G., Grufman, H., et al. (2016). Sphingolipids contribute to human atherosclerotic plaque inflammation. *Arteriosclerosis, Thrombosis, and Vascular Biology, 36*(6), 1132–1140. https://doi.org/10.1161/ATVBAHA.116.305675.

3. Levade, T., Augé, N., Veldman, R. J., Cuvillier, O., Nègre-Salvayre, A., & Salvayre, R. (2001). Sphingolipid mediators in cardiovascular cell biology and pathology. *Circulation Research, 89*(11), 957–968. https://doi.org/10.1161/hh2301.100350.

4. Xu, X., Gao, B., Guan, Q., Zhang, D., Ye, X., Zhou, L., et al. (2016). Metabolomic profile for the early detection of coronary artery disease by using UPLC-QTOF/MS. *Journal of Pharmaceutical and Biomedical Analysis, 129*, 34–42. https://doi.org/10.1016/j.jpba.2016.06.040.

5. Lallemand, T., Rouahi, M., Swiader, A., Grazide, M. H., Geoffre, N., Alayrac, P., et al. (2018). nSMase2 (type 2-neutral sphingomyelinase) deficiency or inhibition by GW4869 reduces inflammation and atherosclerosis in Apoe(-/-) mice. *Arteriosclerosis, Thrombosis, and Vascular Biology, 38*(7), 1479–1492. https://doi.org/10.1161/ATVBAHA.118.311208.

6. Park, T. S., Rosebury, W., Kindt, E. K., Kowala, M. C., & Panek, R. L. (2008). Serine palmitoyltransferase inhibitor myriocin induces the regression of atherosclerotic plaques in hyperlipidemic ApoE-deficient mice. *Pharmacological Research, 58*(1), 45–51. https://doi.org/10.1016/j.phrs.2008.06.005.

7. Wang, D. D., Toledo, E., Hruby, A., Rosner, B. A., Willett, W. C., Sun, Q., et al. (2017). Plasma ceramides, Mediterranean diet, and incident cardiovascular disease in the PREDIMED trial (Prevencion con Dieta Mediterranea). *Circulation, 135*(21), 2028–2040. https://doi.org/10.1161/CIRCULATIONAHA.116.024261.

8. de Carvalho, L. P., Tan, S. H., Ow, G. S., Tang, Z., Ching, J., Kovalik, J. P., et al. (2018). Plasma ceramides as prognostic biomarkers and their arterial and myocardial tissue correlates in acute myocardial infarction. *JACC Basic Translational Science, 3*(2), 163–175. https://doi.org/10.1016/j.jacbts.2017.12.005.

9. Laaksonen, R., Ekroos, K., Sysi-Aho, M., Hilvo, M., Vihervaara, T., Kauhanen, D., et al. (2016). Plasma ceramides predict cardiovascular death in patients with stable coronary artery disease and acute coronary syndromes beyond LDL-cholesterol. *European Heart Journal, 37*(25), 1967–1976. https://doi.org/10.1093/eurheartj/ehw148.

10. Meeusen, J. W., Donato, L. J., Bryant, S. C., Baudhuin, L. M., Berger, P. B., & Jaffe, A. S. (2018). Plasma ceramides. *Arteriosclerosis Thrombosis and Vascular Biology, 38*(8), 1933–1939. https://doi.org/10.1161/ATVBAHA.118.311199.

11. Ali, Z. A., Karimi Galougahi, K., Maehara, A., Shlofmitz, R. A., Ben-Yehuda, O., Mintz, G. S., et al. (2017). Intracoronary optical coherence tomography 2018: current status and future directions. *JACC. Cardiovascular Interventions, 10*(24), 2473–2487. https://doi.org/10.1016/j.jcin.2017.09.042.

12. Burgmaier, M., Milzi, A., Dettori, R., Burgmaier, K., Marx, N., & Reith, S. (2018). Co-localization of plaque macrophages with calcification is associated with a more vulnerable plaque phenotype and a greater calcification burden in coronary target segments as determined by OCT. *PLoS One, 13*(10), e0205984. https://doi.org/10.1371/journal.pone.0205984.

13. Sinclair, H., Bourantas, C., Bagnall, A., Mintz, G. S., & Kunadian, V. (2015). OCT for the identification of vulnerable plaque in acute coronary syndrome. *JACC: Cardiovascular Imaging, 8*(2), 198–209. https://doi.org/10.1016/j.jcmg.2014.12.005.

14. Ibanez, B., James, S., Agewall, S., Antunes, M. J., Bucciarelli-Ducci, C., Bueno, H., et al. (2018). 2017 ESC Guidelines for the management of acute myocardial infarction in patients presenting with ST-segment elevation: The Task Force for the management of acute myocardial infarction in patients presenting with ST-segment elevation of the European Society of Cardiology (ESC). *European Heart Journal, 39*(2), 119–177. https://doi.org/10.1093/eurheartj/ehx393.

15. Jia, H., Abtahian, F., Aguirre, A. D., Lee, S., Chia, S., Lowe, H., et al. (2013). In vivo diagnosis of plaque erosion and calcified nodule in patients with acute coronary syndrome by intravascular optical coherence tomography. *Journal of the American College of Cardiology, 62*(19), 1748–1758. https://doi.org/10.1016/j.jacc.2013.05.071.

16. Monnin, C., Ramrup, P., Daigle-Young, C., & Vuckovic, D. (2018). Improving negative liquid chromatography/electrospray ionization mass spectrometry lipidomic analysis of human plasma using acetic acid as a mobile-phase additive. *Rapid Communications in Mass Spectrometry, 32*(3), 201–211. https://doi.org/10.1002/rcm.8024.

17. Sarafian, M. H., Gaudin, M., Lewis, M. R., Martin, F. P., Holmes, E., Nicholson, J. K., et al. (2014). Objective set of criteria for optimization of sample preparation procedures for ultra-high throughput untargeted blood plasma lipid profiling by ultra performance liquid chromatography-mass spectrometry. *Analytical Chemistry, 86*(12), 5766–5774. https://doi.org/10.1021/ac500317c.

18. Bismuth, J., Lin, P., Yao, Q., & Chen, C. (2008). Ceramide: a common pathway for atherosclerosis? *Atherosclerosis, 196*(2), 497–504. https://doi.org/10.1016/j.atherosclerosis.2007.09.018.

19. Freed, J. K., Beyer, A. M., LoGiudice, J. A., Hockenberry, J. C., & Gutterman, D. D. (2014). Ceramide changes the mediator of flow-induced vasodilation from nitric oxide to hydrogen peroxide in the human microcirculation. *Circulation Research, 115*(5), 525–532. https://doi.org/10.1161/circresaha.115.303881.

20. Schissel, S. L., Tweedie-Hardman, J., Rapp, J. H., Graham, G., Williams, K. J., & Tabas, I. (1996). Rabbit aorta and human atherosclerotic lesions hydrolyze the sphingomyelin of retained low-density lipoprotein. *The Journal of Clinical Investigation, 98*(6), 1455–1464. https://doi.org/10.1172/JCI118934.

J. of Cardiovasc. Trans. Res. (2021) 14:140–149

149

21. Brown, B. A., Williams, H., & George, S. J. (2017). Evidence for the involvement of matrix-degrading metalloproteinases (MMPs) in atherosclerosis. *Progress in Molecular Biology and Translational Science, 147*, 197–237. https://doi.org/10.1016/bs.pmbts.2017.01.004.

22. Thim, T., Hagensen, M. K., Bentzon, J. F., & Falk, E. (2008). From vulnerable plaque to atherothrombosis. *Journal of Internal Medicine, 263*(5), 506–516. https://doi.org/10.1111/j.1365-2796.2008.01947.x.

23. Falk, E. (2006). Pathogenesis of atherosclerosis. *Journal of the American College of Cardiology, 47*(8 Suppl), C7–C12. https://doi.org/10.1016/j.jacc.2005.09.068.

24. Li, H., Junk, P., Huwiler, A., Burkhardt, C., Wallerath, T., Pfeilschifter, J., et al. (2002). Dual effect of ceramide on human endothelial cells. *Circulation, 106*(17), 2250–2256. https://doi.org/10.1161/01.cir.0000035650.05921.50.

25. Reith, S., Milzi, A., Lemma, E. D., Dettori, R., Burgmaier, K., Marx, N., et al. (2019). Intrinsic calcification angle: a novel feature of the vulnerable coronary plaque in patients with type 2 diabetes: an optical coherence tomography study. *Cardiovascular Diabetology, 18*(1), 122. https://doi.org/10.1186/s12933-019-0926-x.

26. Milzi, A., Burgmaier, M., Burgmaier, K., Hellmich, M., Marx, N., & Reith, S. (2017). Type 2 diabetes mellitus is associated with a lower fibrous cap thickness but has no impact on calcification morphology: an intracoronary optical coherence tomography study. *Cardiovascular Diabetology, 16*(1), 152. https://doi.org/10.1186/s12933-017-0635-2.

27. Fretts, A. M., Jensen, P. N., Hoofnagle, A., McKnight, B., Howard, B. V., Umans, J., et al. (2019). Plasma ceramide species are associated with diabetes risk in participants of the strong heart study. *The Journal of Nutrition.* https://doi.org/10.1093/jn/nxz259.

28. Raichur, S., Brunner, B., Bielohuby, M., Hansen, G., Pfenninger, A., Wang, B., et al. (2019). The role of C16:0 ceramide in the development of obesity and type 2 diabetes: CerS6 inhibition as a novel therapeutic approach. *Mol Metab, 21*, 36–50. https://doi.org/10.1016/j.molmet.2018.12.008.

29. Huynh, K. (2016). Coronary artery disease: ceramides predict CV death in stable CAD and ACS. *Nature Reviews Cardiology, 13*(7), 381. https://doi.org/10.1038/nrcardio.2016.81.

30. Janis, M. T., Tarasov, K., Ta, H. X., Suoniemi, M., Ekroos, K., Hurme, R., et al. (2013). Beyond LDL-C lowering: distinct molecular sphingolipids are good indicators of proprotein convertase subtilisin/kexin type 9 (PCSK9) deficiency. *Atherosclerosis, 228*(2), 380–385. https://doi.org/10.1016/j.atherosclerosis.2013.03.029.

31. Ng, T. W., Ooi, E. M., Watts, G. F., Chan, D. C., Weir, J. M., Meikle, P. J., et al. (2014). Dose-dependent effects of rosuvastatin on the plasma sphingolipidome and phospholipidome in the metabolic syndrome. *The Journal of Clinical Endocrinology and Metabolism, 99*(11), E2335–E2340. https://doi.org/10.1210/jc.2014-1665.

32. Tarasov, K., Ekroos, K., Suoniemi, M., Kauhanen, D., Sylvanne, T., Hurme, R., et al. (2014). Molecular lipids identify cardiovascular risk and are efficiently lowered by simvastatin and PCSK9 deficiency. *The Journal of Clinical Endocrinology and Metabolism, 99*(1), E45–E52. https://doi.org/10.1210/jc.2013-2559.